https://doi.org/10.48048/tis.2023.4027

Two-Stage Feature Selection Method Created for 20 Neurons Artificial Neural Networks for Automatic Breast Cancer Detection

Jalpa J. Patel[1,*] and Sarman K. Hadia[2]

[1]V.T. Patel Department of Electronics and Communication Engineering, Chandubhai S. Patel Institute of Technology, Charotar University of Science and Technology, Gujarat, India
[2]Gujarat Technological University, Gujarat, India

([*]Corresponding author's e-mail: jalpajpatel08@gmail.com)

Received: 5 May 2022, Revised: 18 June 2022, Accepted: 25 June 2022, Published: 2 December 2022

Abstract

Breast cancer is a common deadly diseases in women. Initial recognition of breast cancer using mammogram images is a challenging task. Hence, this paper proposed a unique automatic diagnosis model for breast cancer. Initially, the mammogram images are preprocessed with a median filter and contrast limited adaptive histogram equalization (CLAHE). The pre-processed image is automatically segmented using the multilevel threshold method. Subsequently, statistical, texture, shape, and geometric features are extracted from the segmented image. So, the length of the feature vector is high, and it is important to identify optimum features. In this paper, the dimension of the feature vector is reduced by 2-stage feature selection methods. Initially, the feature vector is applied to the best first search method information gain (IG) with rank feature method, and then secondly, apply the Pearson correlation method (PCM). Artificial neural networks (ANNs) are used to increase the classification accuracy of a breast cancer diagnosis. In this model, the selection of appropriate neurons in a single hidden layer is used to avoid overfitting problems in an ANN model. Based on optimum feature selection, the appropriate number of neurons chosen in the hidden layer is 20, which was applied for the proposed IG+PCM+Boosted-ANN model. The proposed model is applied on 2 regular datasets mini-Mammographic Image Analysis Society (mini-MIAS) and Digital Database for Screening Mammography (DDSM). The proposed model was superior to other exiting models and the model in this study achieves the accuracy of 99 and 98.80 % for mini-MIAS and DDSM datasets, respectively.

Keywords: Multi-level threshold, Information Gain, Pearson correlation, Heat map, Boosted-ANN, Automatic Breast Cancer Detection (ABCD), Digital Database for Screening Mammography (DDSM)

Abbreviations:

CLAHE: Contrast Limited Adaptive Histogram Equalization,
ANN: Artificial Neural Networks,
IG: Information Gain,
PCM: Person Correlation Method,
mini-MIAS: Mammographic Image Analysis Society,
DDSM: Digital Database for Screening Mammography,
WDBC: Wisconsin Diagnostic Breast Cancer,
CAD: Computer Aided Diagnosis,
FS: Feature Selection,
ML: Machine Learning,
EML: Extreme Machine Learning Technique,
GLCM: Gray Level Co-occurrence Matrix,
GLRLM: Gray Level Run Length Matrix,
PSO-SVM: Particle Swarm Optimization-Support Vector Machine,
FFBPNN: Feed Forward with Back Propagation Neural Network,
SVM: Support Vector Machine,
LD: Linear Discriminant,
FT: Fine Tree,
DC: Decision Tree,
KNN: K Mean Clustering,
NB: Naïve Bayes,

FC: Fuzzy Classification,
AUC: Area Under the Curve,
ROC: Receiver Operating Curve,
FFNN: Feed Forward Neural Network,
ROIs: Region of Interest,
MLP: Multi-Layer Perceptron,
RF: Random Forest,
CNN: Cellular Neural Network,
MCC: Matthews correlation coefficient,
SRE: Short Run Emphasis,
LRE: Long Run Emphasis,
GLNU: Grey Level Non-uniformity,
RLNU: Run Length Non-uniformity,
LGRE: Low Grey Level Run Emphasis,
HGRE: High Grey level Run Emphasis,
WHC: Women Health Care Program,
FFBPNN: Feed Forward Back Propagation Neural Network,
ABCD: Automatic Breast Cancer Detection

Introduction

In the current year, breast cancer has become one of the most common reasons for death among women. As per the report given by the American Cancer Society, breast cancer cases reach up to 2, 52, 710 among women in the US in 2017, and it has been seen harmful cell is generally perilous. The passing rate is required to be 40,610 in 2017. The condition is horrible in a less evolved country like India. According to a Globocan report, breast cancer is common cancer in India and 1, 62, 468 new cases were identified each year and the demise rate is 87,090 per year [1,2]. Thus, it is most important to reduce the breast cancer death rate through timely detection and viable treatment.

The actual recognition of showing mammograms by radiologist is tedious, expensive, and time-consuming reasons of negative rates. Notwithstanding, variety in tissue and the absence of expertise make the recognition process difficult. To overcome these issues, ABCD systems need to be developed by dedicated computer systems which can support radiologists to identify the correct lesion [3]. The primary goal of the CAD system is to deal with the automatically correlated to a healthy and abnormal lesions of mammogram images. The role of the CAD framework is to distinguish, automatically identify and separate the abnormal lesions [4].

FS has become an important technique, especially in bioinformatics, where it's in various applications. ML might be amazing which will choose the outstanding most applicable elements from datasets; however, not all ML algorithms perform similar to first search methods. In a classification problem, FS remains the most superior task. So, to increase classification accuracy FS is an important method. The 3 sorts of FS methods- filter, wrapper, and embedded methods, are used for optimum-feature selection for the classification model [5].

ANN plays a significant role in the field of medical science to solve health issues and diagnose several diseases. For an accurate diagnosis, FFBPNN is used to minimize errors [6]. A nested Ensemble technique is used for pattern recognition and automatic diagnosis of breast tumors [7,8].

In image processing, ML and ANNs algorithms for recognition and classification of masses in digital mammograms would be a simple approach, yet at the same time, it is a difficult task to study. This paper focuses on an effective technique for FS, the number of neurons selected in ANN, and the classification of masses in digital mammogram images. The primary target of the FS procedure is to eliminate co-linear or repetitive features, to improve the classification accuracy.

The significant commitments of this research are as per the following:

To improve an advanced ABCD model using the following steps: (i) pre-processing, (ii) segmentation, (iii) feature extraction, (iv) feature selection, and (v) ANN Classification.

1) The input mammogram image is pre-processed using a median filter and CLAHE. The pre-processed image is an automatically segmented using a multi-level threshold.

2) From the segmented image, the features are extracted during the feature extraction phase, and the optimum features are subjected to classification in the machine learning and ANN classifier, for binary classification.

3) The selected feature is applied to the proposed ANN model so that the accuracy is maximum. At last, the IG+PCM+Boosted-ANN model is compared with the current algorithms like SVM, FT, NB, LR, KNN, LD, and ensemble tree by analyzing accuracy, specificity, precision, recall, F1-score, AUC, and MCC.

The entire association of the article is defined as follows: Section 2 represents the related work on exiting breast cancer methodologies. Section 3 shows the proposed method of breast cancer recognition. Section 4 gives the optimum feature selection and classification methodology for breast cancer detection. Section 5 shows the results and discussions, and Section 6 concludes the paper.

In this work, there were 3 challenges to (i) automatic segmentation to diagnose breast cancer, (ii) determining the optimum features, and (iii) the number of neurons selected of improving ANNs.

Related works

In the earlier decade, a less CAD models have been proposed for screening mammogram images. The classification is based on 4 main issues such as segmentation, feature extraction, feature selection, and classification models. The majority of the work reported up till now utilizes freely accessible datasets, namely mini- MIAS and DDSM [9,10]. Using the first search technique has become critical in many classification problems. By less numbers of features set are used to improve the performance of the algorithm [11-13].

Qayyum *et al.* [14] proposed an automatic segmentation for ROI. The texture features were extracted from the ROIs. They used an SVM classifier to identify normal and abnormal mammogram images from the mini-MIAS dataset. The proposed method got an accuracy of 96.55 % with a sensitivity of 96.97 % and a specificity is 96.29 %. Mohamed *et al.* [15] proposed automatic segmentation for the WHC and DDSM datasets. According to shape features, segmented masses were classified. For lobular and uneven shapes got 93 and 100 % accuracy using the ANN-based classification on the WHC database. Furthermore, for the DDSM database, the technique got accuracies of 100.0 and 91.3 %, respectively.

Fatih [16] has introduced a comparative analysis for breast cancer detection using ML algorithms including LR, KNN, SVM, NB, DT, RF, and rotation forest. The analysis is carried out using Minitab, R, and Python were chosen to be applied to these ML algorithms for the Wisconsin dataset. Finally got the highest accuracy of 98.1 % for the LR model. Kaur *et al.* [17] have presented an ABCD using feature extraction by K-mean clustering using Speed-Up Robust Features (SURF). They applied 10-fold cross-validation for SVM, LD, KNN, and DT to achieve the accuracy of 96.9, 93.8, 89.7 and 88.7 %, respectively.

Shravya *et al.* [18] proposed model for supervised machine learning. This research was implemented on classifiers like Logistic Regression, SVM and KNN. The dataset was downloaded from UCI repository and results were conducted with respect to performance. According to this, SVM was a good classifier and it gave 92.7 % accuracy on the python platform. Mohanty *et al.* [19] proposed forest optimization used for FS. Different classifiers such as SVM, KNN, Naïve Bayes, and C4.5 were used to classify normal and abnormal mammogram lesions. The authors used the MIAS dataset and achieved a maximum accuracy of 97.86 % for the Naïve Bayes classifier.

In 2019, Chisto *et al.* [20] proposed ensemble feature selection for 2 different types of datasets Hepatitis and WDBC. In this proposed method, 10-fold cross-validation technique is used, to train BPNN is used and got the classification accuracy of 98.47 and 95.51 % for WDBC and Hepatitis datasets, respectively. Chtihrakkannan *et al.* [21] have used, wavelet transforms to find out first-order features and second order based GLCM. In this method, X-ray mammogram images are used as input Images. They used deep neural network as a classifier and got average accuracy of 89.77 % with higher sensitivity of 93.22 %.

Alyami *et al.* [22] have presented accurate diagnoses using SVM and ANN for high classification accuracy. For feature selection, the correlation coefficient method is used to remove irrelevant features. They used a WDBC dataset with a 10-Fold Cross-validation technique and a number of selected features were applied to the classifier. And achieved an accuracy of 97.14 % for SVM and 96.71 % for ANN.

In 2018, Thawkar *et al.* [23] defined an automatic segmentation using a seed-based region growing technique for breast lesion detection and for precisely diagnosing, the optimal threshold generated by swarm optimization techniques. Texture features are extracted using GLCM and GLRCM. Several features are applied to the FFNN algorithm to recognize malignant and benign masses. Punitha *et al.* got a sensitivity of 98.1 % with a specificity of 97.8 % for the DDSM database. In 2018, Erika *et al.* [24] proposed an automatic segmentation for mini-MIAS and DDSM datasets. For segmentation morphological operations were applied including image decomposition and interpolation. Erika *et al.* got an accuracy of 94.48 % for

the DDSM and 100 % for the mini-MIAS datasets. **Table 1** represents the challenges, methods, and number of features used in previous work.

Table 1 Methodology and challenges of expected diagnoses of breast cancer methods.

Authors	Method	Database	Features	Challenges
[11] Elkhani *et al.*	Binary particle swarm optimization feature selection	Microarray cancer data	Nine modeling steps	Time computation high
[13] Gao *et al.*	IG+SVM	Gene expression datasets	Filter irrelevant and redundant genes	Performance is superior as evaluated using 5 cancer gene expression
[14] Qayyum *et al.*	SVM 1340482	MIAS	Identify normal and abnormal masses Texture Feature Extracted	Accuracy is high
[16] Fatih	LR, KNN, SVM,NB,RF, DT, Rotation Forest	WDBC	Analysis has been carried out with different software	Achieve high accuracy
[19] Mohanty *et al.*	EML	MIAS	Contourlet features are extracted from ROIs	Feature selection based on forest optimization
[21] Chtihrakkannan *et al.*	Deep Neural Network	X-ray mammogram images	Feature Selection based on Wavelet Transform	Time complexity less and Numbers of features are extracted
[22] Alyami *et al.*	SVM, ANN	WDBC	Feature selection based on correlation coefficient	High classification Accuracy
[23] Thawkar *et al.*	FFNN	MIAS and DDSM	To diagnose accuracy Guide to a radiologist for initial detection	Region growing algorithm
[24] Erika *et al.*	MC (Micro calcification cluster) segmentation	MIAS and DDSM	Decomposition and Interpolation	Achieve high accuracy Contrast Enhancement filter used to remove noise

Datasets and methodology

Dataset

In this paper we are using 2 different types of datasets: The first one is from the mini-MIAS database in the United Kingdom. It comprises 322 mammogram images which are characterized into normal, cancerous, and non-cancerous classes. The size of the image was reduced for the MIAS database by 1,024×1,024. In this database, 208 mammograms are normal, while the other 115 indicate unhealthy. In this paper, image numbers mb258, mb260 and mb297 are not considered because of the poor quality of the images. Secondly, DDSM has a total of 2,620 cases; out of them, 673 mammogram images are used. In this database, 405 mammogram images are normal while 268 mammogram images are abnormal. The DDSM images are in Joint Photographic Experts Group format with different sizes and different resolutions.

Methodology

The proposed model benefits from an automatic diagnostic method for breast cancer classification. **Figure 1** shows a diagram representation of automatic breast cancer identification.

Image Pre-processing; Initially remove undesirable parts or unessential regions from the related mammogram images. It also removes noise from these images. For that, we are using a median filter for the pre-processed image.

Image Enhancement; It is a processing for the mammogram images to increase contrast and defeat noise, to assist radiologists to identify irregularities of the suspicious region. For improving the contrast of this grayscale image, we have used CLAHE [25]. **Figure 2** shows a histogram representation of the

suspicious lesion. **Figure 2(c)** shows that the gray level ranges i.e. between 150 to 170 the frequency is high, so it is easy to identify abnormal mass for a particular image.

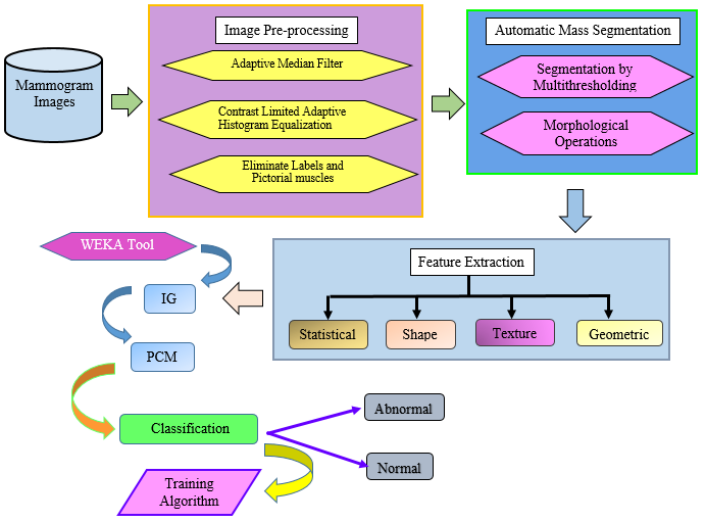

Figure 1 Diagram for proposed automatic diagnosis of breast cancer identification.

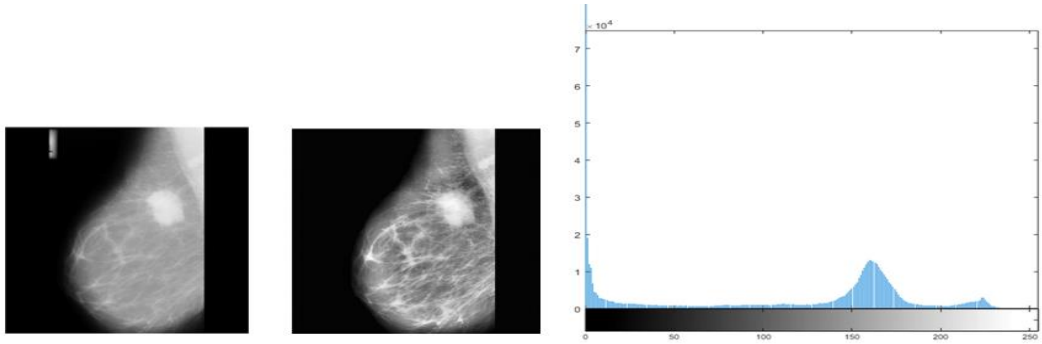

Figure 2 (a) Original image (b), Enhanced mammogram image, and (c) Histogram representation of enhanced image.

Image Segmentation; Doubtful masses are automatically segmented from the mammogram images. The lesion tends to be brighter than the encompassing region, thus they have more intensity values. Multilevel threshold based on Otsu's technique segment a grayscale image over a couple of several free regions. In this process, gray-level images are separated into sets or classes dependent on their intensity level. This process selects more than 1 threshold value for the actual image and segments the image into a certain bright area, which is correlated to 1 background and more than a few substances. Pixels regions covering the highest label values of size varying from 300 to 22,000 pixels are chosen. For that, we are utilizing morphological functions opening and closing [26,27].

1) Morphological operation

To remove unwanted regions, morphological operations are very useful [26]. The main purpose is to accurate information of the image with a lesser geometric pattern called a structural element. Here, for removing the additional parts and also improved the quality of the image, 3 morphological operations were used "opening", "closing" and "filling holes" using Eqs. (1) - (3);

$$A \odot B = (A \odot B) \oplus B \quad (1)$$

where S defines the structural element (in this paper disk element is selected with a '5' radius).

$$A \odot B = (A \odot B) \ominus B \quad (2)$$

The third morphological function is accurate filling which can be utilized for filling the empty holes in the threshold image. This process is reached by the below equations;

$$Z_K = (Z_{K-1} \oplus S) \cap A^C \quad k = 1,2,3 \ldots \quad (3)$$

Figure 3 shows simulated results of the image segmentation of the mammogram images. Here, **Figure 3(a)** shows an original mammogram image which is having an abnormal lesion with a binary mask image shown in **Figure 3(b)** (Binary Mask_1). In **Figure 3(c)** is an enhanced image with the suspicious lesion. For removing extra parts or labels of the enhanced image shown in **Figure 3(d)** (Mask Image) and **Figure 3(e)** (Pictorial_Image_1). In this image shows that the background area is suppressed with high contrast region. This indicates that the targeted region is clearly visible. **Figure 3(f)** (Segmented Image_1); shows the segmented region from the original image.

Figure 4 shows original normal images pre-processed with pictorial removed images and automatic segmentation. For normal mammogram image segmentation, it looks like a scatter of that image. So, we can identify that it's a normal image.

Figures 5 and **6** shows simulated results from the mini-MIAS and the DDSM database with automatic image segmentation of the mammogram images. **Figures 5(d) - 5(h)** and **Figure 6(d)** are clearly visible to identify an abnormal mass of particular images. **Figure 7** shows the automatically segmented image for the model applied in [28].

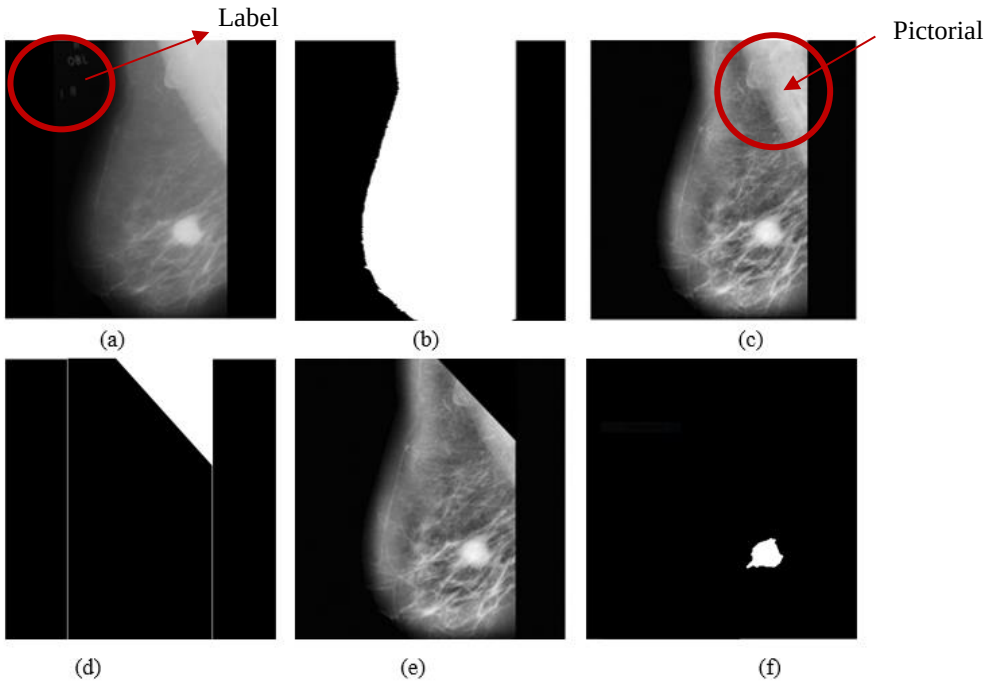

Figure 3 Original mammogram image with binary mask and Enhanced mammograms with pictorial removed muscles and segmented image part. (a) Mam_1, (b) Binary Mask_1, (c) Enhanced_1, (d) Upper_Triagle_ image_1, (e) Pictorial removed image_1, and (f) Segmented image_1.

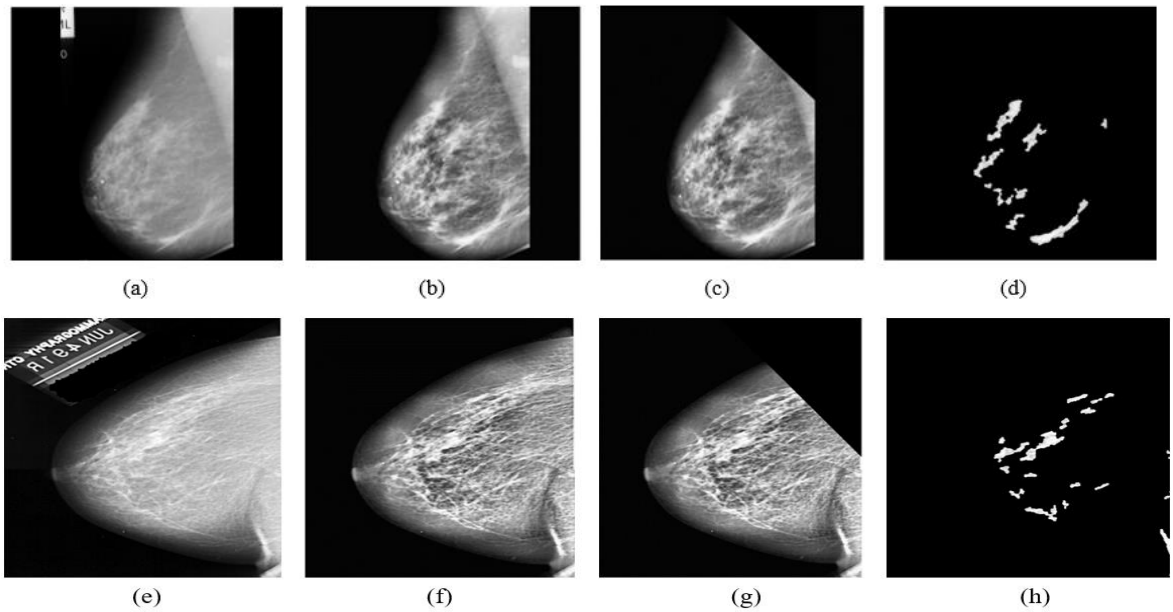

Figure 4 Original normal images with enhanced mammograms with pictorial removed muscles and segmented image (a), (e) Mam_2, (b), (f) Enhanced_2, (c), (g) Pictorial removed imag_2 (d), (h) Segmented image_2.

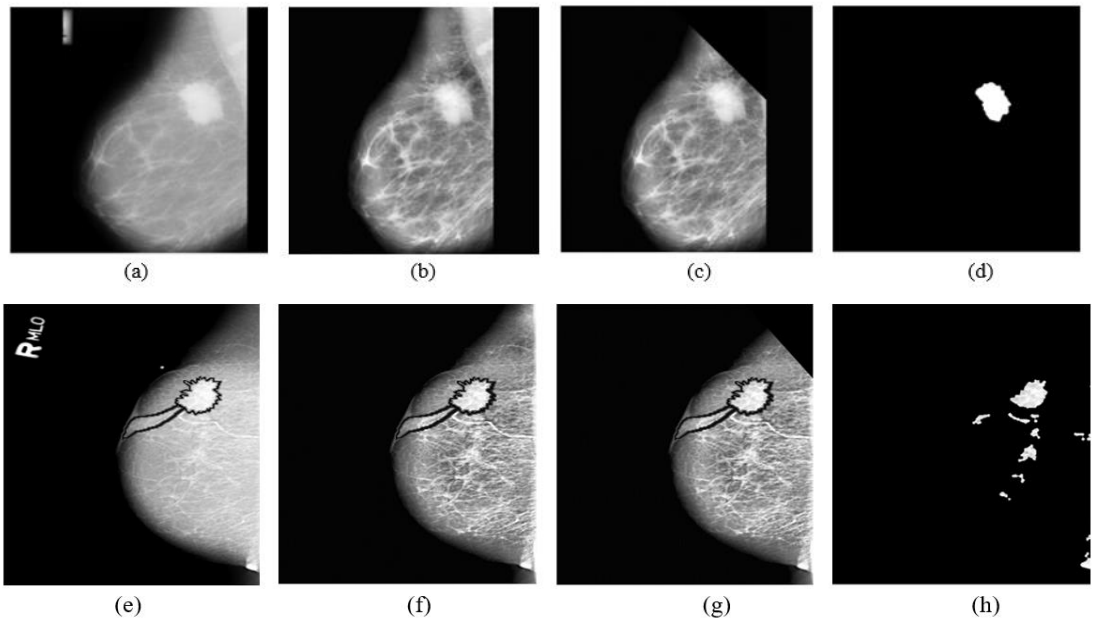

Figure 5 Original abnormal image with enhanced mammograms with pictorial removed muscles and segmented image part. (a), (e) Mam_2, (b), (f) Enhanced_2, (c), (g) Pictorial removed imag_2 (d), (h) Segmented image_2.

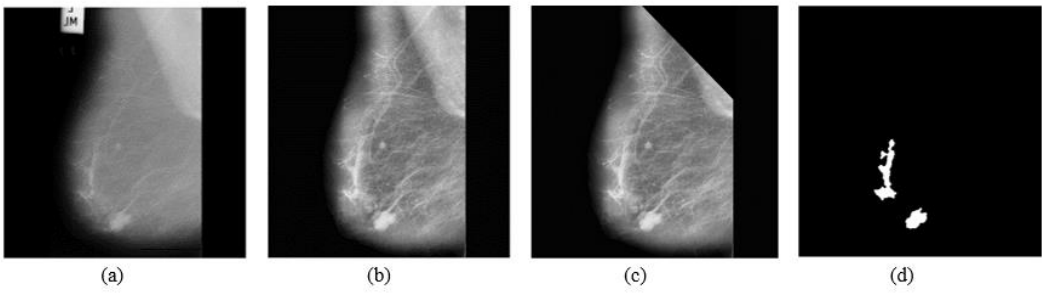

Figure 6 Original abnormal image with enhanced mammograms with pictorial removed muscles and segmented image. (a) Mam_2, (b) Enhanced_2, (c) Pictorial removed imag_2, and (d) Segmented image_2.

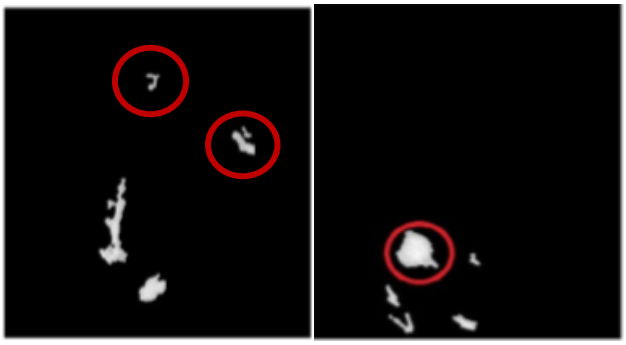

Figure 7 Automatic segmented mammogram images of the model [28].

Feature extraction; Feature extraction shows an important role in classification.

1) Statistical feature method

In this process, the power of the intensity level is based histogram of the image to define the gray level intensity features. Statistical features are extracted from the segmented images-mean, standard deviation, variance, skewness, kurtosis, energy, and entropy. These types of features are utilized to approximate the brightness, contrast, and intensity dissimilarity of the segmented region. In mammogram images mass tends to be brighter and have high contrast as compared to normal tissues, the statistical features are useful to identify doubtful masses. Higher Contrast signifies ordinary tissues of an image.

2) Shape-based method

The shape and edge of mass are important to identify them as considered normal, cancerous, and non-cancerous. 5 shape-based features have been identified from the segmented image. These types of attributes are helping to identify the lesion and its irregularity. It also includes area, perimeter, circularity, compactness, uniformity, roundness, and solidity.

3) Second order gray level co-occurrence matrix method

It is one of the techniques to secure the second-order features is to define the probability of a connection among 2 pixels a ways off and unique direction. There are more than a few stages for the second order, the first forming of the matrix co-occurrence and another is specific characteristics as a function of the matrix. GLCM is a technique to determine an enormous set of second-order texture features and 16 features are carried out along with ɵ is 0, 45, 90 and 135 ° with distance d=1 utilized and orientation in degree for all mammogram images. In this paper, various types of texture features are extracted from GLCM [29]. **Figure 8** shows that GLCM features are carried out from the segmented image and all features are based on texture analysis. It is an important part of detecting the presence of abnormalities of masses. We can also identify texture features like texture mean, texture Global mean, texture Standard deviation, texture Smoothness, texture entropy, texture Skewness and texture correlation [29]. The sample image input consists of 8 gray levels. GLCM represents the relation between reference pixel (j) and neighbor pixel (i) at various angles.

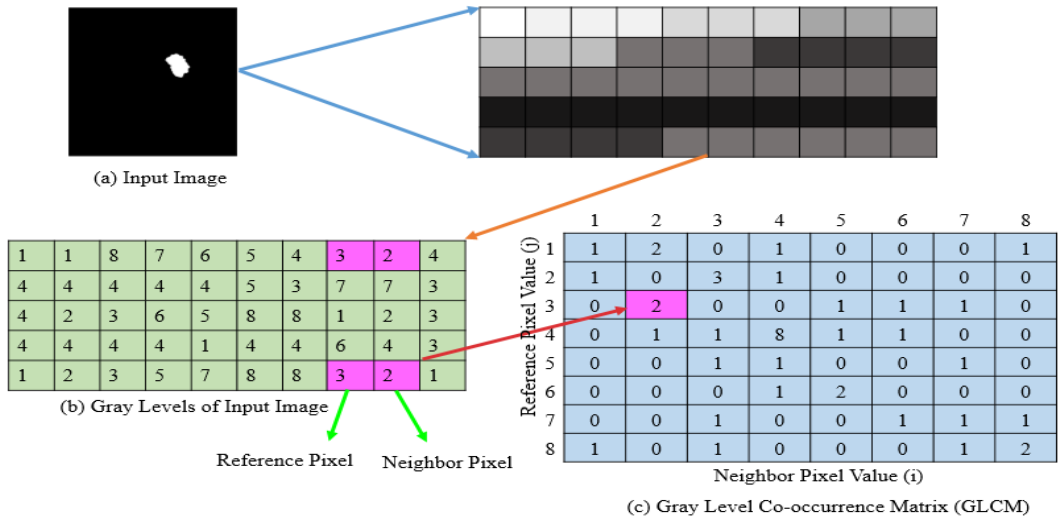

Figure 8 Gray level co-occurrence matrix from segmented image.

4) Geometric based feature method

These features are seen as feasible in separating cancerous and healthy lesions. This is because of the way that both healthy and unhealthy lesions appear from 1 spot and improve circumferentially. **Figure 3** shows the segmented region for our proposed method to separate geometric shape features like geometric area, geometric perimeter, geometric compactness and also global mean [30].

5) Grey level run length matrix method

This technique is an analysis of a statistical way that searches the image for the runs of pixels taking the same gray level values in a number specific direction θ using the GLRLM derived from the segmented image [31]. It is the number of runs with pixels of gray level I and run-length j for a particular direction. It is a texture representation method to extract higher-order statistical values related to each pixel. To extract 6 attributes from the GLRLM. The GLRLM features include SRE, LRE, GLNU, RLN, LGRE, and HGRE. These features play a significant role in separating normal mass which has evenly distributed texture as compared to abnormal mass which has binary textures mammogram image I (i, j) is the matrix to find the GLRLM features based on the below Eqs. (31) - (32). The total number of features extracted from a segmented mammogram is 44. **Table 2** shows statistical, shape and texture features.

Table 2 Intensity, Shape and texture features.

Intensity features	Texture features
Mean $$Mean(\mu) = \sum_{i,j=0}^{n-1} I(i,j)$$	Energy $$Energy = \sum_{i=1}^{m}\sum_{j=1}^{n} I(i,j)^2$$
Variance $$Variance\ \sigma i^2 = \sum_{i,j=0}^{n-1} I(i,j)\,(i - \mu i)^2$$	Entropy $$Entropy = -\sum_{i=1}^{m}\sum_{j=0}^{n-1} I(i,j) log I(i,j)$$
Standard Deviation $$Standard\ Deviation(\sigma) = \sigma i = \sqrt{\sigma i^2}$$	Contrast $$Contrast = \sum_{i=1}^{m}\sum_{j=1}^{n} I(i,j)\lvert i-j\rvert^2$$

Intensity features	Texture features
Skewness $skewness = \frac{\sum_{i=1}^{m}\sum_{j=1}^{n} I(i,j) - \mu^3}{m * n * \sigma^2}$ Kurtosis $kurtosis = \frac{\sum_{i=1}^{m-1}\sum_{j=1}^{n-1} I(i,j) - \mu^4}{m * n * \sigma^4}$	Correlation $= \frac{\sum_{i=0}^{m-1}\sum_{j=0}^{n-1} I(i,j)\frac{1}{1+(i-j)^2} I(i,j) - \mu i \mu j}{\sigma i \sigma j}$ $Homogeneity = \sum_{i=0}^{m-1}\sum_{j=0}^{n-1}\frac{1}{1+(i-j)^2} I(i,j)^2$ Short Run Emphasis (SRE) $SRE = \sum_{i=1}^{m}\sum_{j=1}^{n}\frac{I(i,j)}{j^2}$ Long Run Emphasis (LRE) $LRE = \sum_{i=1}^{m}\sum_{j=1}^{n} j^2 I(i,j)$
Shape Features	
Area $Area\ (A) = \pi r^2$ Perimeter $Perimeter = 2\pi r$ Compactness $Compactness = \frac{4\pi A}{P^2}$	Grey Level Non-uniformity (GLNU) $GLNU = \sum_{i=1}^{m}\left[\sum_{j=1}^{n} I(i,j)\right]^2$ Run Length Non-uniformity (RLNU) $RLNU = \sum_{i=1}^{m}\left[\sum_{j=1}^{n}\frac{I(i,j)}{j^2}\right]^2$ Low Grey Level Run Emphasis (LGRE) $LGRE = \sum_{i=1}^{m}\sum_{j=1}^{n}\frac{I(i,j)}{i^2}$ High Grey level Run Emphasis (HGRE) $HGRE = \sum_{i=1}^{m}\sum_{j=1}^{n} i^2 I(i,j)$

Feature selection (FS); It is a method that can decrease data dimension; it also includes the collection of the best appropriate subset of the main extracted attribute. This paper utilized a 2-stage procedure to select the appropriate features. The first search technique was the initial step, and the second step was the person correlation method. Those attributes commonly appear in positive and negative classes only. 29 most important features are extracted using these 2 methods.

IG: For the IG calculates for all features through WEKA, compare the entropy of the input dataset and also check the rank for each feature. The high rank for each feature is arranged according to feature ranking [33]. The feature ranking stage focuses on ranking the subsets of features by high information gain entropy in decreasing order.

PCM: In this method, extracted features are used in python to calcite correlation calculates each feature. According to a heat map, we set the threshold value as 0.9 which means above 0.9 which are most correlated features. So, out of them, we can use only use 1 feature. In this heat map, negative values are also available. We cannot ignore this negative value because it represents the most important features. **Figure 9** represent the heat map for DDSM and mini-MIAS datasets. After the final assessment, only the 24 most appropriate features were identified for breast cancer classification. **Figure 10** shows the feature selection model for this proposed method.

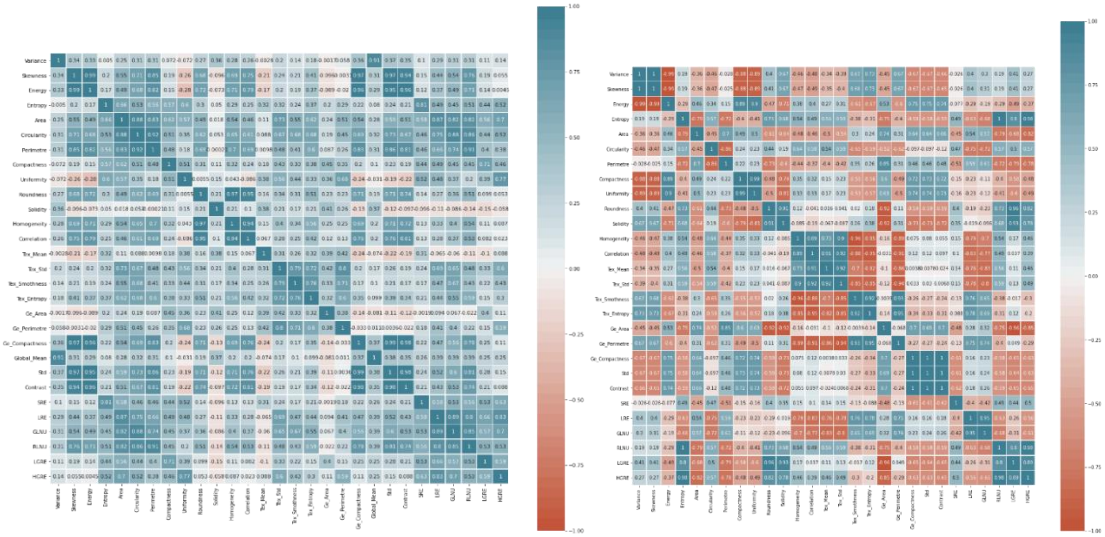

Figure 9 (a) Heat map for DDSM database and (b) Heat map for mini-MIAS database.

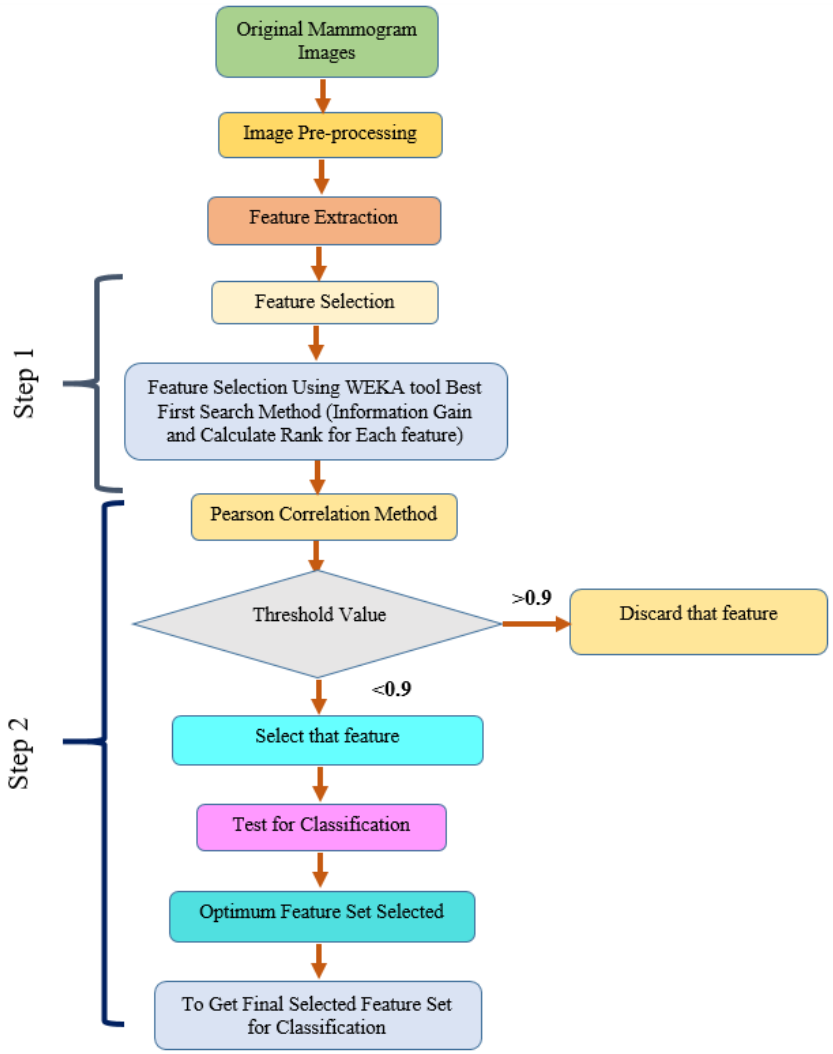

Figure 10 Feature selection model.

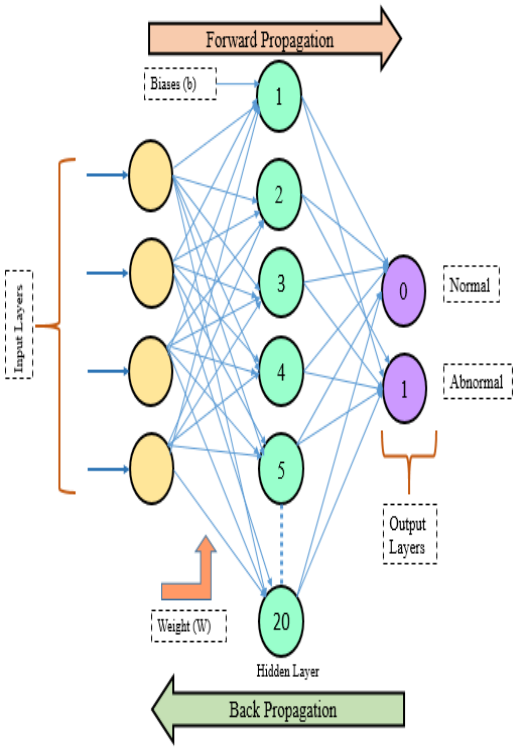

Figure 11 Design of the proposed 20 neurons ANN with binary output.

Classification approach

The ANN; Recently, for solving several types of technical and scientific problems artificial intelligence (AI) is used. AI covers intellectuals' structure that signifies or imitate social abilities to solve the problem. ANNs is solving various types of problems, including classification problems. The ANN is an ML methodology, with the human brain interconnected with artificial neurons. In ANN neurons have lesser contacts compared to a biological structure. **Figure 11** shows the proposed ANN architecture.

The proposed NN model with FFBP takes the lowest processing nodes called neurons or processing elements. To get the output, the sigmoid activation function is used for inputs and connected with weights and numbers of neurons using Eq. (4). During back propagation the connected weights are adjusted correspondingly and reduce error. At the training stage, weight values are very with the network. The number of weights defines the link connected from 1 layer of neurons to other. Henceforth, variations in the changing the values on input and output, along with changes in weight values [34].

$$\emptyset(x) = \frac{1}{1+e^{-x}} \quad (4)$$

The design of a Multi-layer FFBPNN system is shown in **Figure 11**, it contains more than 1 input layer and more than 1 hidden layer along with the output layer [35]. The Proposed Boosted-ANN model has 20 neurons in a single hidden layer for diagnosing breast cancer classification. To find out appropriate numbers of neurons specific for this breast cancer classification model is called Boosted-ANNs. So, this type of proposed ANN covers 3 stages: Data Collection, Pre-Processing, Segmentation, Feature Extraction, Feature Selection, data upload in MATLAB tool, data partition, ANN training-testing-validation and applicable to find out the best partition and number of the neuron is used particularity for this proposed Boosted-ANN.

All selected attributes from an automatic segmented images are applied in the Pattern Recognition Tool of MATLAB (R2019b). This attribute divided into 3 parts: Training, Testing and Validation. Most of the neural networks are trained with Gradient descent because it adjusts the learning rate and minimizes the objective function. **Tables 3** and **4** shows the number of neurons available in a single hidden layer neural network for MIAS and DDSM datasets, respectively and partition. By this method, numbers of hidden layers are selected randomly until excellent accuracy was obtained for training and testing datasets. At 20 neurons get excellent performance and it is sufficient to build Boosted-ANN model for diagnosis of breast cancer shown in **Figure 12**.

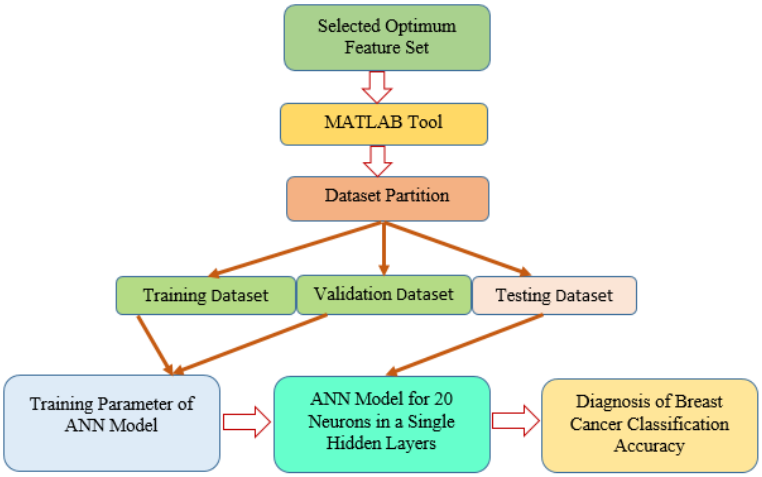

Figure 12 The proposed Boosted-ANN Model with 20 neurons in a single hidden layers.

The mini-MIAS and DDSM datasets were arbitrarily separated into 3 parts: Training, testing and validation. These parts separated into 4 groups: First: 50, 25, 25 %; Second: 60, 20, 20 %; Third, 70, 15, 15 %; and Fourth: 80, 10, 10 %. It has been shown that in **Tables 3** and **4** first experiment, we divide these whole datasets 50 % to train the model, 25 % for validation, and the rest 25 % for testing. The highest accuracy for mini-MIAS and DDSM datasets is 98.90 and 98.20 %, respectively for a single hidden layer for 20 neurons. If we increase the number of neurons performance is reduced significantly and also the performance of the ANN model is negative.

In the second trial, datasets were separated into 60 % for training, 20 % for validation, and the rest of 20 % for testing. The performance of the Boosted-ANN model is increased by 0.30 and 0.10 % for mini-MIAS and DDSM datasets, respectively. In the third experiment, the datasets were divided into 70, 15 and 15 % for training, validation, and testing, respectively. In this experiment, the highest accuracy achieves for 99.24 and 98.50 % for mini-MIAS and DDSM datasets, respectively.

Finally, in the last experiment, the datasets divide into 80 % for training, 10 % for validation, and the rest of 10 % for testing. In this experiment, accuracy is decreased by 0.34 and 2.10 % for mini-MIAS and DDSM datasets, respectively. All the experiments have shown that at 20 neurons we will get the highest training and testing accuracy in the proposed Boosted-ANN model breast cancer classification. Here, using a single hidden layer, got very good accuracy for the both datasets. Table 5 shows that, If we increase numbers of hidden layers, model complexity is increase and the performance of the proposed model may decrease.

Table 3 ANN to choose the appropriate number of neurons for breast cancer detection for MIAS dataset.

First	Training accuracy (%)	Validation accuracy (%)	Testing accuracy (%)	Partition of dataset		
Number of neurons chosen				Training (%)	Validation (%)	Testing (%)
10	97.20	97.90	96.50			
12	97.90	97.20	94.40			
14	98.00	97.90	93.70			
16	98.10	97.90	93.40			
18	95.80	97.20	96.00			
19	98.80	98.60	95.10			
20	98.90	98.10	96.80			
21	97.90	96.50	95.10	50	25	25
22	98.60	96.50	96.50			
24	98.50	96.60	95.10			
25	98.10	98.01	94.80			

Second	Training accuracy (%)	Validation accuracy (%)	Testing accuracy (%)	Partition of dataset		
Number of neurons chosen				Training (%)	Validation (%)	Testing (%)
10	97.40	96.50	97.40			
12	97.90	96.00	98.20			
14	97.70	97.40	96.50			
16	96.80	98.20	98.20			
18	96.80	98.20	93.90			
19	96.50	97.40	95.60			
20	99.20	95.60	98.50			
21	98.20	96.50	97.40	60	20	20
22	98.80	96.50	94.70			
24	98.10	98.20	98.20			
25	97.20	98.20	96.50			
Three	**Training accuracy (%)**	**Validation accuracy (%)**	**Testing accuracy (%)**	**Partition of dataset**		
Number of neurons chosen				**Training (%)**	**Validation (%)**	**Testing (%)**
10	98.20	99.30	95.80			
12	98.00	96.50	95.30			
14	96.70	95.30	97.60			
16	97.50	96.50	97.60			
18	97.20	97.60	95.30			
19	98.50	98.80	98.50			
20	99.24	98.00	98.90			
21	98.00	96.50	97.60	70	15	15
22	97.70	96.50	98.70			
24	97.20	97.60	96.50			
25	98.20	96.50	94.10			
Four	**Training accuracy (%)**	**Validation accuracy (%)**	**Testing accuracy (%)**	**Partition of dataset**		
Number of neurons chosen				**Training (%)**	**Validation (%)**	**Testing (%)**
10	95.00	96.50	94.70			
12	96.20	98.20	98.20			
14	95.50	96.50	98.10			
16	96.70	100.0	96.50			
18	97.10	94.70	94.70			
19	93.00	94.70	96.50			
20	98.90	100.0	98.30			
21	97.60	100.0	94.70	80	10	10
22	95.20	93.00	96.50			
24	97.90	100.0	97.30			
25	97.80	100.0	96.50			

Table 4 ANN to choose the appropriate number of neurons for breast cancer detection for DDSM dataset.

First	Training accuracy (%)	Validation accuracy (%)	Testing accuracy (%)	Partition of dataset		
Number of neurons chosen				Training (%)	Validation (%)	Testing (%)
10	97.60	97.20	96.20	50	25	25
12	96.40	97.60	98.50			
14	98.20	97.00	94.00			
16	97.00	97.60	95.80			
18	97.90	99.40	96.40			
19	98.01	97.00	97.50			
20	98.20	97.20	98.80			
21	97.00	99.40	98.20			
22	97.60	97.00	95.20			
24	96.70	96.40	97.00			
25	96.10	97.60	97.60			
Second	**Training accuracy (%)**	**Validation accuracy (%)**	**Testing accuracy (%)**	**Partition of dataset**		
Number of neurons chosen				**Training (%)**	**Validation (%)**	**Testing (%)**
10	96.80	95.60	94.80	60	20	20
12	98.30	96.30	97.00			
14	98.00	97.80	97.80			
16	97.80	97.80	97.80			
18	97.80	97.00	97.00			
19	97.30	95.60	95.60			
20	98.30	95.60	99.40			
21	98.00	97.00	97.00			
22	96.50	97.80	97.70			
24	98.00	93.30	93.30			
25	97.30	97.80	95.60			
Three	**Training accuracy (%)**	**Validation accuracy (%)**	**Testing accuracy (%)**	**Partition of dataset**		
Number of neurons chosen				**Training (%)**	**Validation (%)**	**Testing (%)**
10	98.30	93.10	96.00	70	15	15
12	98.50	99.00	95.00			
14	97.20	95.00	100.0			
16	99.20	98.00	96.00			
18	98.70	96.00	99.00			
19	98.90	99.00	97.10			
20	98.50	97.00	99.40			
21	96.80	96.00	99.00			
22	96.80	99.00	99.00			

24	98.30	97.00	98.90			
25	97.50	98.00	98.00			
Four	**Training accuracy (%)**	**Validation accuracy (%)**	**Testing accuracy (%)**	**Partition of dataset**		
Number of neurons chosen				**Training (%)**	**Validation (%)**	**Testing (%)**
10	93.20	94.00	94.00	80	10	10
12	95.50	98.50	98.50			
14	94.10	95.50	95.50			
16	93.40	98.50	98.50			
18	95.90	98.50	98.50			
19	94.30	98.50	97.00			
20	96.40	97.00	98.80			
21	93.70	98.50	97.00			
22	92.70	97.00	98.50			
24	94.70	98.50	97.00			
25	92.00	98.30	97.20			

Table 5 Different number of hidden layers and different accuracies of validation and testing outputs.

Number of hidden layer	**MIAS database**		**DDSM database**	
	Validation accuracy (%)	**Testing accuracy (%)**	**Validation accuracy (%)**	**Testing accuracy (%)**
1	100	99.00	98.30	99.50
2	99.5	98.9	97.60	94.10
3	97.7	97.9	94.10	93.60

Performance Evaluation Criteria for Proposed Improved-ANN classifier model; The classifier performance depends on numerous aspects such as accuracy, sensitivity, specificity, precision, MCC, F1-score and AUC. All these values calculate using a confusion matrix, as shown in **Table 6** below.

Table 6 Confusion matrix for binary classification.

Predicted Class		**Positive**	**Negative**
	Positive	TP	FP
	Negative	FN	TN

True class

TP: True Positive; FP: False Positive; FN; False Negative; TN: True Negative

Eq. (5) was used to calculate classification accuracy.

$$Accuracy = \frac{TP+TN}{TP+FP+TN+FN} \quad (5)$$

Identification for a true positive sample for these 2 classifier is called sensitivity. It is achieved using Eq. (6).

$$Sensitivity/Recall = \frac{TP}{TP+FN} \quad (6)$$

For calculating negative sample for this classification called specificity. Eq. (7) was used to calculate this.

$$Specificity = \frac{TN}{TN+FP} \quad (7)$$

The number of positive case predictions that truly belong to the positive case defines by Eq. (8).

$$Precision = \frac{TP}{TP+FP} \quad (8)$$

F1- score gives a single score value concerns precision and recall in a single number. Eq. (9) is used for calculating the F1- score.

$$F1 - score = 2 * \frac{Precision*Recall}{Precision+Recall} \quad (9)$$

In ML, we can also measure the MCC of the superiority of the 2 classes. MCC value is between −1 to +1 and it is obtained by Eq (10).

$$MCC = \frac{(TP*TN)-(FP*FN)}{\sqrt{(TP+FN)(TN+FP)(TP+FP)(TN+FN)}} \quad (10)$$

The true positive rate (TPR) and false-positive rate (FPR) are recognized with their correlation by the ROC curve. It can improve classification, as its threshold value may vary. The ROC curve is formed by plotting TPR against FPR. AUC shows the perfect outcome for the classification. The AUC is nearer to 1 which means the accuracy of the model is high and its less than 0.5 accuracy for this classification model is less. Eq. (11) was used to calculate AUC. (8).

$$AUC = \frac{1}{2}\left(\frac{TP}{TP+FN} + \frac{TN}{TN+FP}\right) \quad (11)$$

Results and discussion

The proposed model was tested on MATLAB (R2019b) with Core-i5, the 3.4 GHz processor. 12 GB RAM and the window-10 operating system. The suitable number for a single hidden layer is 20 neurons. The proposed model has experimented on mini-MIAS and DDSM datasets. In **Tables 7** and **8** shows the results of 20 different classification simulation using mini-MIAS and DDSM, respectively with their equivalent percentage errors. The average testing accuracies were 98.79 % for the mini-MIAS dataset and 98.02 % for the DDSM dataset. The percentage error for MIAS and DDSM datasets were 0.9 and 1.7 %, respectively.

Table 7 Proposed model classification accuracy based on 20 trial for mini-MIAS dataset.

Number of trial	Training accuracy (%)	Validation accuracy (%)	Testing accuracy (%)	Error (%)
1	99.60	98.50	99.00	1.0
2	99.60	97.20	98.90	1.1
3	99.70	98.50	98.30	1.7
4	99.60	98.80	100.0	0.0
5	99.50	98.50	99.50	0.5
6	99.20	99.60	99.60	0.4
7	99.00	97.60	99.90	0.1
8	98.20	97.90	98.90	1.1
9	98.10	100.0	97.50	2.5

Number of trial	Training accuracy (%)	Validation accuracy (%)	Testing accuracy (%)	Error (%)
10	98.30	98.80	99.60	0.4
11	99.20	98.80	98.70	1.3
12	99.00	98.90	98.60	1.4
13	99.20	98.70	98.80	1.2
14	98.50	98.60	99.10	0.9
15	99.00	98.10	100.0	0.0
16	98.70	98.60	98.90	1.1
17	98.50	98.50	98.50	1.5
18	98.60	100.0	99.10	0.9
19	98.70	98.60	98.80	1.2
20	99.60	98.60	99.90	0.1
Average	98.99	98.64	98.79	0.9

Table 8 Proposed model classification accuracy based on 20 trail for DDSM dataset.

Number of trial	Training accuracy (%)	Validation accuracy (%)	Testing accuracy (%)	Error (%)
1	98.70	96.00	98.00	2.0
2	97.90	97.30	98.30	1.7
3	99.20	98.00	97.10	2.9
4	97.90	97.00	98.80	1.2
5	98.30	98.00	97.80	2.2
6	96.80	100.0	97.20	2.8
7	96.90	98.00	97.60	2.4
8	97.90	98.30	98.60	1.4
9	96.60	97.00	98.50	1.5
10	98.10	97.50	98.80	1.2
11	98.70	98.10	98.00	2
12	98.50	97.50	97.60	2.4
13	98.70	97.60	98.20	1.8
14	96.00	98.00	98.60	1.4
15	97.50	100.0	99.60	0.4
16	97.90	99.00	98.90	1.1
17	98.90	99.20	97.70	2.3
18	98.90	98.10	98.20	1.8
19	98.30	96.50	98.00	2.0
20	98.90	97.50	98.80	1.2
Average	98.03	97.93	98.02	1.7

Figures (13) - **(18)** show that the Boosted-ANN model, training performance of the cross-entropy, performance of the training state, histogram of an error, confusion matrix for classification accuracy, ROC curve for the mini-MIAS dataset. **Figure 13** shows that Boosted -ANN training performance of a cross-entropy gives the best performance 0.0018528 at epoch 33 iterations. **Figure 14** shows network training

state performance at epoch 39, the gradient is 0.0082779. The error of a histogram for training, validation and testing data are shown with 20 bins in **Figure 15** specify that the proposed model handle data positively as the error is close to zero. **Figure 16** show that the receiver operating curve shows that cancerous and non-cancerous samples obtained the maximum AUC. **Figure 17** shows MATLAB output for the confusion matrix for training including validation dataset. According to that accuracy reached 99.4 % showing that this system performed very well and had 0.6 % misclassified during its training phase from the proposed Boosted-ANN model. **Figure 18** is a performance confusion matrix for the testing dataset. According to that accuracy reached 99.0 % showing that the model performance is very well and had 1 % misclassified during its testing stage from the proposed Boosted -ANN model.

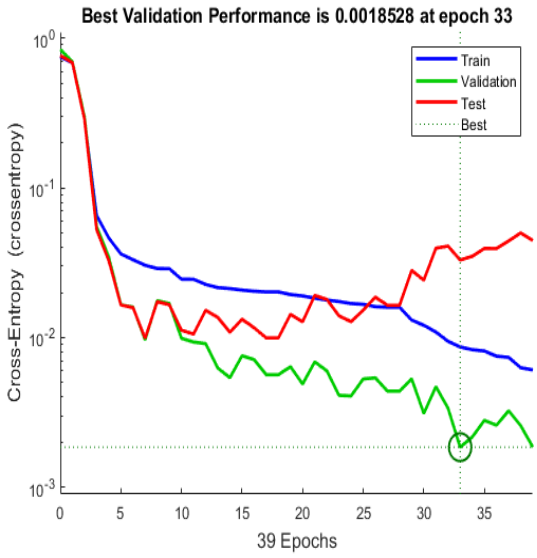

Figure 13 Novel-ANN training performance.

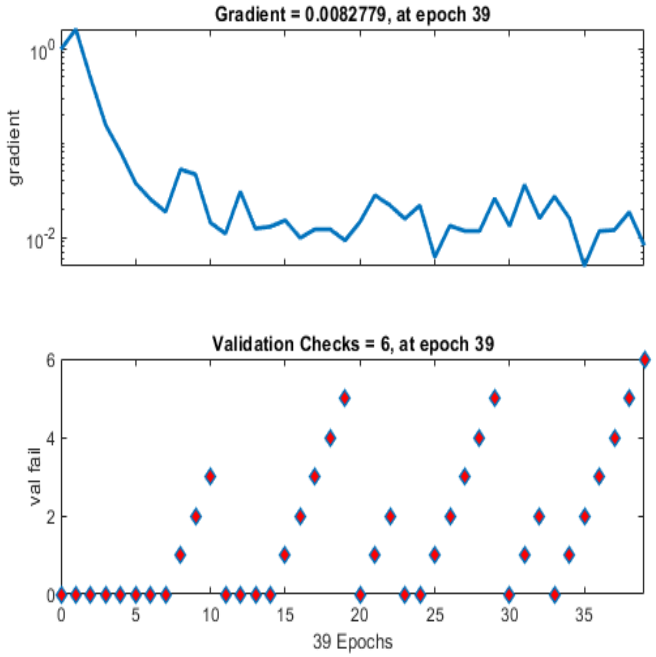

Figure 14 Training state performance.

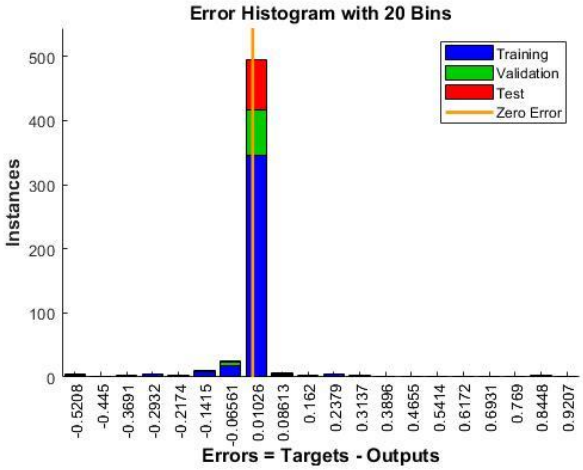

Figure 15 Error histogram.

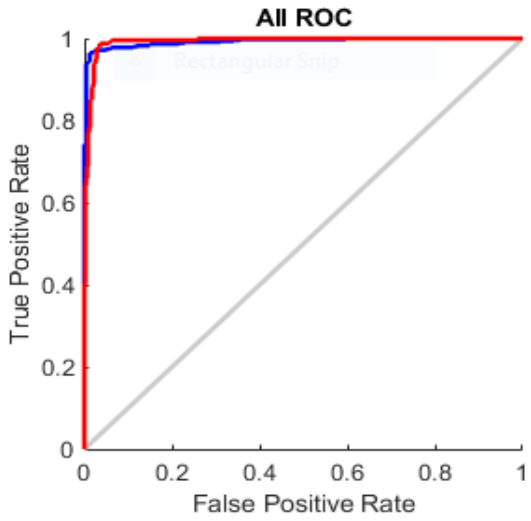

Figure 16 Receiver operating charactristic (ROC) curve.

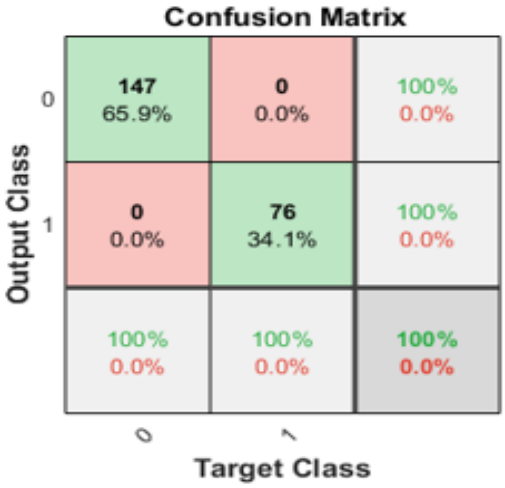

Figure 17 Performance confusion matrix for training including validation.

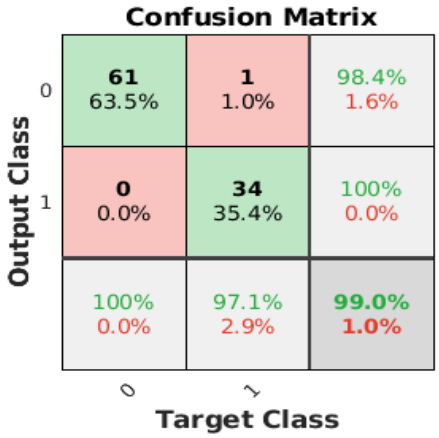

Figure 18 Performance confusion matrix for testing.

Figures (19) - (24) show that the Boosted-ANN model, training performance of the cross-entropy, performance of the training state, histogram of an error, confusion matrix for this binary classification, ROC curve for the DDSM dataset. In **Figure 19** show that the Boosted-ANN training performance of the exact cross-entropy gives the best performance of 0.013721 at epoch 36 iterations. **Figure 20** shows that training state performance at epoch 42, the gradient is 0.02227. The error of a histogram for training, validation and testing data are shown with 20 bins in **Figure 21** shows that the error of the histogram is nearer to zero. **Figure 22** shows that the receiver operating curve shows that cancerous and non-cancerous samples obtained the maximum AUC. **Figure 23** shows MATLAB output for the confusion matrix for training including validation datasets. According to the confusion matrix accuracy reached 98.3 % showing that this system performed very well and had 1.7 % misclassified throughout this training phase from the proposed Boosted- ANN model. **Figure 24** shows that the confusion matrix for testing datasets and accuracy reached 99.5 %.

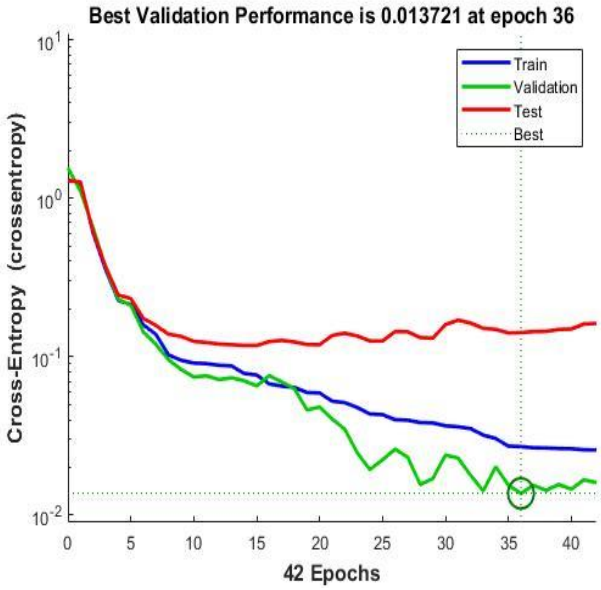

Figure 19 Novel-ANN training performance.

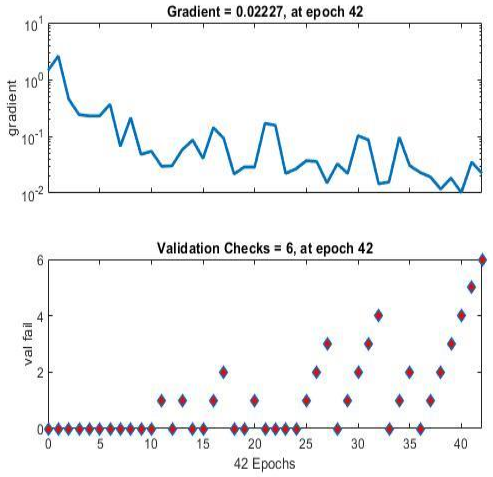

Figure 20 Training state performance.

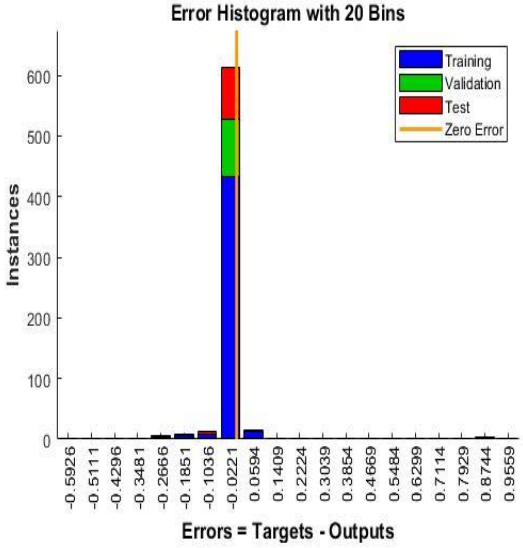

Figure 21 Error histogram.

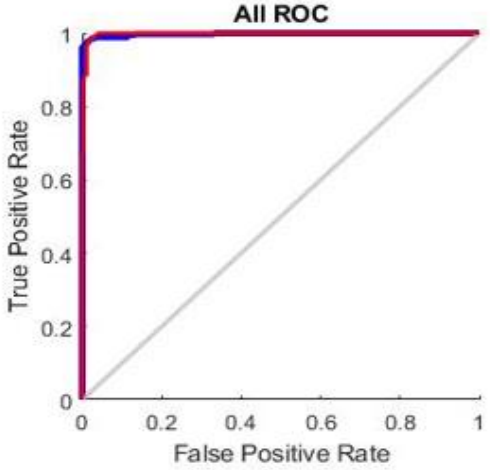

Figure 22 Receiver operating charactristic (ROC) curve.

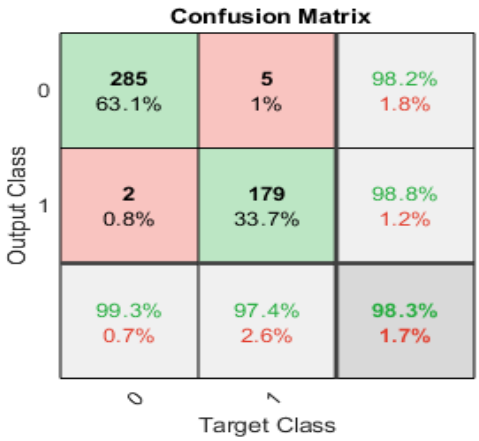

Figure 23 Performance confusion matrix for training including validation.

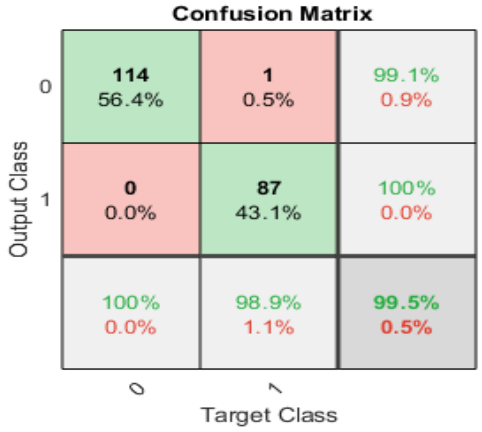

Figure 24 Performance confusion matrix for testing.

Table 9 show that performance obtain from confusion matrix from **Figures 17** - **18** for mini-MIAS training dataset accuracy, sensitivity, specific, precision, F-score, MCC and AUC is 99.70, 99.30, 100, 100, 99.65, 98.43, 100 %, respectively while testing dataset accuracy, sensitivity, specific, precision, F1-score, MCC and AUC are 99, 100, 97.14, 98.39, 99.19, 97.46, 99 %, respectively. **Table 10** show that performance obtain from confusion matrix from **Figures 21** - **22** for DDSM training dataset accuracy, sensitivity, specific, precision, F1-score, MCC and AUC is 98.30, 99.30, 87.28, 98.28, 98.79, 96.86, 98 %, respectively while testing dataset accuracy, sensitivity, specific, precision, F-score, MCC and AUC are 99.50, 100, 98.86, 99.13, 99.56, 99.00, 99 %, respectively.

Table 9 Model performance based on confusion matrix for MIAS dataset.

Dataset	Accuracy (%)	Sensitivity (%)	Specificity (%)	Precision (%)	F1-Score (%)	MCC (%)	AUC (%)
Training dataset	99.70	99.30	100	100	99.65	98.43	100
Testing dataset	99.00	100	97.14	98.39	99.19	97.46	99.00

Table 10 Model performance based on confusion matrix for DDSM dataset.

Dataset	Accuracy (%)	Sensitivity (%)	Specificity (%)	Precision (%)	F1-Score (%)	MCC (%)	AUC (%)
Training dataset	98.30	99.30	97.28	98.28	98.79	96.86	98.00
Testing dataset	99.50	100	98.86	99.13	99.56	99.00	99.00

Table 11 shows that the different stat of art models compare with the proposed IG+PCM+ Boosted -ANN model for both datasets. Performance evaluation was recognized using the MATLAB classification learner tool for the diagnosis of breast cancer datasets. All machine learning algorithms give good classification accuracy, but the proposed model gives optimal accuracy. **Figure 25** shows the training time comparison for both the datasets with some of the machine learning algorithms, and it gives very less computation time to train our proposed model.

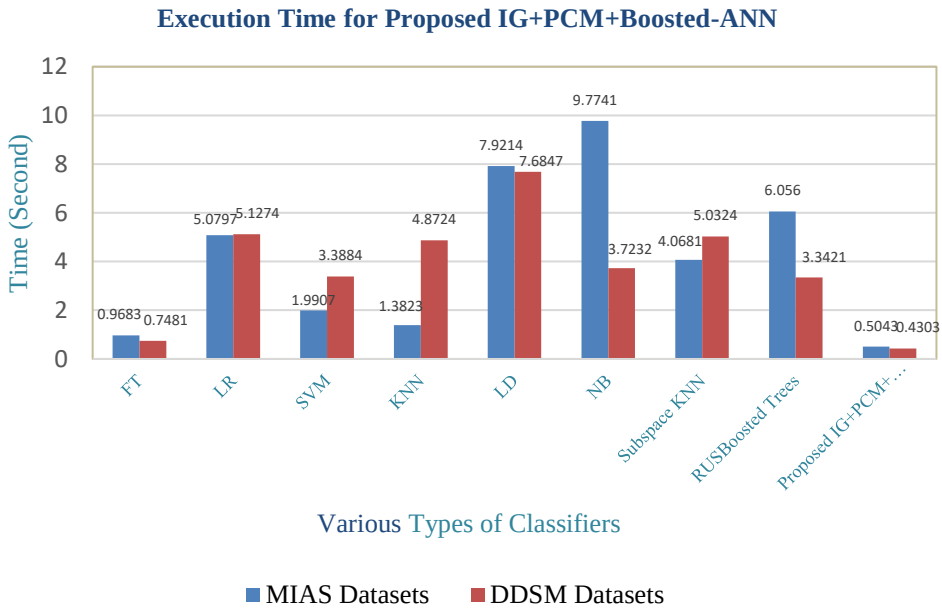

Figure 25 Execution time for proposed IG+PCM+Boosted-ANN.

Table 11 Comparison with state-of-art models with the proposed model for breast cancer detection for mini-MIAS and DDSM datasets.

Classification model	Mini-MIAS dataset		DDSM dataset	
	Validation accuracy (%)	Testing accuracy (%)	Validation accuracy (%)	Testing accuracy (%)
Fine Tree	94.55	93.50	91.50	97.00
Medium Tree	94.51	93.40	91.50	97.02
Coarse Tree	92.30	93.50	92.60	93.60
Linear Discriminant	92.27	91.92	96.20	95.50
Quadratic Discriminant	93.64	94.95	95.80	96.50
Logistic Regression	97.73	96.70	94.50	97.50

Classification model	Mini-MIAS dataset		DDSM dataset	
	Validation accuracy (%)	Testing accuracy (%)	Validation accuracy (%)	Testing accuracy (%)
Gaussian Naïve Bayes	67.01	66.40	93.02	93.10
Kernel Naïve Bayes	64.09	76.77	94.10	94.10
Linear SVM	98.03	97.50	97.50	98.00
Quadratic SVM	98.00	97.00	97.10	97.10
Cubic SVM	97.50	96.97	96.90	97.50
Fine Gaussian SVM	97.00	96.50	90.40	90.60
Medium Gaussian SVM	96.30	97.02	96.60	98.00
Coarse Gaussian SVM	85.20	80.30	96.40	97.50
Fine KNN	90.45	89.90	96.00	97.00
Medium KNN	87.73	94.95	96.40	97.50
Coarse KNN	93.4	92.30	96.20	96.40
Cosine KNN	94.4	95.00	96.30	96.50
Cubic KNN	97.80	98.00	96.60	98.00
Weighted KNN	95.00	96.30	97.00	98.50
Boosted Trees	63.40	66.20	59.90	58.90
Bagged Trees	99.55	97.38	95.10	98.00
Subspace Discriminant	96.36	96.00	96.00	96.10
Subspace KNN	60.20	58.50	92.60	97.00
Boosted Trees	84.30	86.50	94.10	96.50
Proposed IG+PCM+Boosted-ANN	99.70	99.00	98.30	99.50

Table 12 shows that the proposed method has been compared in this context of breast cancer classification based on existing methods with similar datasets. Saleem [36] proposed a convolution neural network classification method with a cheat sheet for classical features to extract from the ROI and got an accuracy of 7.3 % lesser than the proposed method. Dheeba *et al.* [37] proposed particle swarm optimization neural networks for mini-MIAS dataset and achieved good accuracy that is 93.67 %. Devid *et al.* [38] proposed a SVM algorithm approach and achieved 98.8 % correctly classifying the sample. Pratiwi *et al.* [39] proposed feature selection based on the GLCM method for the same datasets and got the accuracy, sensitivity and specificity were 93.90, 97.20 and 91.50 %, respectively. Pezeshki *et al.* [40] used ANN approaches and got an accuracy of 61 % which is very less as compare to this proposed model. Gupta *et al.* [41] used a deep learning technique using Adam gradient descent accuracy achieved 1.16 % lesser than the proposed method. Charaborty *et al.* [42] achieved a 92.5 % accuracy, 93 % with sensitivity and 85 % specificity. Tatikonda *et al.* [43] used MLP for classification and they achieve accuracy of 93.37 % with a sensitivity of 92.43 % and a specificity of 94.18 % which less compared to this proposed model. This comparison table achieved the highest classification accuracy for the mini-MIAS dataset 99.4 % with 99.51 % sensitivity and 99.13 % specificity. And for the DDSM dataset accuracy achieved 98.8 % with 99.50 sensitivity and 97.79 % specificity. In **Table 11** N.A. means data not provided.

Table 12 Comparison of breast cancer diagnosis with existing methods and the proposed boosted-ANN model.

Author name with reference	Classification method	Accuracy (%)	Sensitivity (%)	Specificity (%)
Ramadan Saleem [36]	CNN	92.1	91.4	96.8
Dheeba *et al.* [37]	PSOWNN	93.67	92.11	94.17
Omondiagbe *et al.* [38]	SVM with RBF	98.8	98.41	99.07
Pratiwi *et al.* [39]	GLCM	93.90	97.20	91.50
Pezeshki *et al.* [40]	ANN	61	77	95.03
Gupta *et al.* [41]	Deep Learning	98.24	N.A.	N.A.
Chakraborty *et al.* [42]	Automatic Edge Detection	92.5	93.0	85.0
Tatikonda *et al.* [43]	MLP	93.37	92.43	94.18
The proposed	IG+PCM+Boosted-ANN	99.40	99.51	99.13
		98.80	99.50	97.79

Conclusions

The main objective of this research is to identify classification accuracy to improve image-based diagnosis. This research work focuses on FS to decrease attributes and reached high classification accuracy for breast cancer diagnosis. The proposed 2-stage FS method selected the 24 most important attributes from 44 in both mini-MIAS and DDSM datasets. Secondly, the proposed Boosted-ANN is used to optimize the hidden layer parameter of the ANN model. The experimental results proved that 20 is the optimum number of neurons for a single hidden layer of ANN, and can get the classification accuracy for the training, testing, and validation of designated attributes. In this paper, the proposed Boosted-ANN method reported an overall 99.40 % classification accuracy with 99.51 sensitivity and 99.13 specificity for mini-MIAS dataset and 98.80 % classification accuracy with 99.50 % sensitivity and 97.79 % specificity for the DDSM dataset.

References

[1] H Sung, J Ferlay, RL Siegel, M Laversanne, I Soerjomataram, A Jemal and F Bray. Global cancer statistics 2020: GLOBOCAN estimates of incidence and mortality worldwide for 36 cancers in 185 countries. *CA Canc. J. Clinicians* 2021; **71**, 209-49.

[2] American Cancer Society. *Breast cancer facts & figures 2017-2018*. American Cancer Society, Inc., Georgia, 2017.

[3] H Cheng, X Cai, X Chen, L Hu and X Lou. Computer-aided detection and classification of microcalcifications in mammograms: A survey. *Pattern Recogn.* 2003; **36**, 2967-91.

[4] S Gupta, PF Chyn and MK Markey. Breast cancer cadx based on bi-rads descriptors from two mammographic views. *Med. Phys.* 2006; **33**, 1810-17.

[5] TN Lal, O Chapelle, J Weston and A Elisseeff. *Embedded methods*. Feature Extraction. Springer, Berlin, Germany, 2006, p. 137-65.

[6] MB Wadhonkar, PA Tijare and SN Sawalkar. Artificial neural network approach for classification of heart disease dataset. *Int. J. Appl. Innovat. Eng. Manag.* 2014; **3**, 388-92.

[7] N Elkhani and RC Muniyandi. Review of the effect of feature selection for microarray data on the classification accuracy for cancer data sets. *Int. J. Soft Comput.* 2016; **11**, 334-42.

[8] R Gururajan, XH Tao and PD Barua. A new nested ensemble technique for automated diagnosis of breast cancer. *Pattern Recogn. Lett.* 2020; **132**, 123-31.

[9] J Parker, D Dance, S Astley, I Hutt, C Boggis, I Ricketts, E Stamatakis, N Cerneaz, S Kok, P Taylor, D Betal and J Savage. *Mammographic image analysis society (MIAS) database v1.21*. Apollo - University of Cambridge Repository, Trinity Ln, Cambridge, 2015.

[10] M Heath, K Bowyer, D Kopans, P Kegelmeyer, R Moore and K Chang. *Current status of the digital database for screening mammography*. Digital Mammography. Springer, Berlin, Germany, 1998, p. 457-60.

[11] E Naeimeh and MR Chandren. Membrane computing inspired feature selection model for microarray cancer data. *Intell. Data Anal.* 2017; **21**, S137-57.
[12] MA Rahman and RC Muniyandi. An enhancement in cancer classification accuracy using a two-step feature selection method based on artificial neural networks with 15 neurons. *Symmetry* 2020; **12**, 271.
[13] L Gao, M Ye, X Lu and D Huang. Hybrid method based on information gain and support vector machine for gene selection in cancer classification. *Dev. Reprod. Biol.* 2017; **15**, 389-95.
[14] A Qayyum and A Basit. Automatic breast segmentation and cancer detection via svm in mammograms. *In*: Proceedings of the 2016 International Conference on Emerging Technologies, Islamabad, Pakistan. 2016.
[15] BA Mohamed, NM Salem, MM Hadhoud and AF Seddik. Automatic segmentation and classification of masses from digital mammograms. *Eur. J. Appl. Sci.* 2016; **4**, 17.
[16] MF Ak. A comparative analysis of breast cancer detection and diagnosis using data visualization and machine learning applications. *Healthcare* 2020; **8**, 111.
[17] P Kaur, G Singh and P Kaur. Intellectual detection and validation of automated mammogram breast cancer images by multi-class SVM using deep learning classification. *Informat. Med. Unlocked* 2019; **16**, 100239.
[18] C Shravya, K Pravalika and S Subhani. Prediction of breast cancer using supervised machine learning techniques. *Int. J. Innovat. Tech. Exploring Eng.* 2019; **8**, 1106-10.
[19] F Mohanty, S Rup, B Dash, B Majhi and MNS Swamy. Mammogram classification using contourlet features with forest optimization-based feature selection approach. *Multimed. Tool. Appl.* 2019; **78**, 12805-34.
[20] VRE Christo, HK Nehemiah, B Minu and A Kannan. Correlation-based ensemble feature selection using bioinspired algorithms and classification using backpropagation neural network. *Comput. Math. Meth. Med.* 2019; **2019**, 7398307.
[21] R Chtihrakkannan, P Kavitha, T Mangayarkarasi, R Karthikeyan. Breast cancer detection using machine learning. *Int. J. Innovat. Tech. Exploring Eng.* 2019; **8**, 3123-6.
[22] R Alyami, J Alhajjaj, B Alnajrani, I Elaalami, A Alqahtani, N Aldhafferi, TO Owolabi and SO Olatunji. Investigating the effect of correlation based feature selection on breast cancer diagnosis using artificial neural network and support vector machines. *In*: Proceedings of the 2017 International Conference on Informatics, Health & Technology, Riyadh, Saudi Arabia. 2017.
[23] S Thawkar and R Ingolikar. Classification of masses in digital mammograms using Biogeography-based optimization technique. *J. King Saud Univ. Comput. Inform. Sci.* 2020; **32**, 1140-8.
[24] R Erika, EDN Alam, A Oliver and R Zwiggelaar. Automatic segmentation of microcalcification clusters. *In*: Proceedings of the Annual Conference on Medical Image Understanding and Analysis, Southampton. 2018.
[25] N Kharel, A Alsadoon, PWC Prasad and A Elchouemi. Early diagnosis of breast cancer using contrast limited adaptive histogram equalization (CLAHE) and morphology methods. *In*: Proceedings of the 2017 8th International Conference on Information and Communication Systems, Irbid, Jordan. 2017.
[26] Y Zhang, TY Ji, MS Li and QH Wu. Identification of power disturbances using generalized morphological open-closing and close-opening undecimated wavelet. *IEEE Trans. Ind. Electron.* 2018; **63**, 2330-9.
[27] Q Chen, L Zhao, J Lu, G Kuang, N Wang and Y Jiang. Modified two-dimensional Otsu image segmentation algorithm and fast realization. *IET Image Process.* 2012, **6**, 426-33.
[28] KU Sheba and SG Raj. An approach for automatic lesion detection in mammograms. *Cogent Eng.* 2018; **5**, 1444320.
[29] JJ Patel and SK Hadia. An enhancement of mammogram images for breast cancer classification using artificial neural networks. *IAES Int. J. Artif. Intell.* 2021; **10**, 332-45.
[30] AK Mohanty, S Beberta and SK Lenka. Classifying benign and malignant mass using GLCM and GLRLM based on textures from mammogram. *Int. J. Eng. Res. Appl.* 2011; **1**, 687-93.
[31] P Zarbakhsh and A Addeh. Breast cancer tumor type recognition using graph feature selection technique and radial basis function neural network with optimal structure. *J. Canc. Res. Therapeut.* 2018; **14**, 625-33.
[32] PT Bharathi and P Subashini. Texture based color segmentation for infrared river ice images using K-means clustering. *In*: Proceedings of the 2013 International Conference on Signal Processing, Image Processing & Pattern Recognition, Coimbatore, India. 2013.
[33] F Amiri, MR Yousefi and C Lcas. Mutual information based feature selection for intrusion detection system. *J. Netw. Comput. Appl.* 2011; **34**, 1184-99.

[34] M Sepandi, M Taghdir, A Rezaianzadeh and RS Assessing. Breast cancer risk with an artificial neural network. *Asian Pac. J. Canc. Prev.* 2018; **4**, 1017-9.
[35] MA Rahman, R Muniyandi, D Albashish, MM Rahman and OL Usman. Artificial neural network with Taguchi method for robust classification model to improve classification accuracy of breast cancer. *PeerJ Comput. Sci.* 2021; **7**, e344.
[36] SZ Ramadan. Using convolutional neural network with cheat sheet and data augmentation to detect breast cancer in mammograms. *Comput. Math. Meth. Med.* 2020; **2020**, 9523404.
[37] J Dheeba, NA Singh and ST Selvi. Computer-aided detection of breast cancer on mammograms: a swarm intelligence optimized wavelet neural network approach. *J. Biomed. Informat.* 2014; **49**, 45-52.
[38] DA Omondiagbe, S Veeramani and AS Sidhu. Machine learning classification techniques for breast cancer diagnosis. *IOP Conf. Mater. Sci. Eng.* 2019; **495**, 012033.
[39] M Pratiwi, Alexander, J Harefa and S Nanda. Mammograms classification using gray-level co-occurrence matrix and radial basis function neural network. *Procedia Comput. Sci.* 2015; **59**, 83-91.
[40] H Pezeshki, M Rastgarpour, A Sharifi and S Yazdani. Extraction of spiculated parts of mammogram tumors to improve accuracy of classification. *Multimed. Tool. Appl.* 2019; **78**, 19979-20003.
[41] P Gupta and S Garg. Breast cancer prediction using varying parameters of machine learning models. *Procedia Comput. Sci.* 2016; **171**, 593-601.
[42] S Chakraborty, MK Bhowmik, AK Ghosh and T Pal. Automated edge detection of breast masses on mammograms. *In*: Proceedings of the 2016 IEEE Region 10 Conference, Singapore. 2016.
[43] KC Tatikonda, CM Bhuma and SK Samayamantula. The analysis of digital mammograms using HOG and GLCM features. *In*: Proceedings of the 2018 9th International Conference on Computing, Communication and Networking Technologies, Bengaluru, India. 2018.